J Comput Aided Mol Des (2008) 22:773–781
DOI 10.1007/s10822-008-9212-9

WARR'S PIECE

Investigation of structures and properties of cyclic peptide nanotubes by experiment and molecular dynamics

Jingchuan Zhu · Jie Cheng · Zhouxiong Liao · Zhonghong Lai · Bo Liu

Received: 22 November 2007 / Accepted: 18 March 2008 / Published online: 2 April 2008

Abstract In order to investigate the structures and properties of cyclic peptide nanotubes of cyclo[(-D-Phe-L-Ala)$_{n\,=\,3,4,5,6}$-], *cyclo*[(-D-Phe-L-Ala)$_{n\,=\,4}$-] was synthesized and self-assembled to nanotubes, and its structure and morphology of the nanotube were characterized by mass spectrometry (MS), fourier transform infrared spectroscopy (FT-IR) and scanning electron microscopy (SEM). On the basis of these experimental results, the structures of *cyclo*[(-D-Phe-L-Ala)$_{n\,=\,3,4,5,6}$-] were characterized by molecular dynamics. In addition, the motion behaviors of H_2O molecules in nanotubes were investigated by molecular dynamics using a COMPASS force field. Experimental results show that *cyclo*[(-D-Phe-L-Ala)$_{n\,=\,4}$-] peptides self-assemble into nanotube bundles. Molecular modeling results indicate that cyclic peptide nanotubes with $n = 3$, 4, 5 and 6 are very stable; these nanotubes have internal diameters of 5.9 Å, 8.1 Å, 10.8 Å and 13.1 Å and outer diameters of 18.2 Å, 21.7 Å, 23.4 Å and 25.9 Å respectively. Modeling results demonstrate that H_2O molecules move in cooperation in single nanotube and they diffuse in one dimension, but they did not diffuse unilaterally due to the antiparallel ring stacking arrangement.

J. Zhu (✉) · J. Cheng (✉) · Z. Liao · Z. Lai
School of Materials Science and Engineering, Harbin Institute of Technology, Box 433, No. 92 West Dazhi Street, Harbin 150001, P.R. China
e-mail: t.j.cheng@163.com

B. Liu
School of Chemical and Environmental Engineering, Harbin University of Science and Technology, No. 52, Xuefu Road, Box 128, Harbin 150040, P.R. China

Keywords Cyclic peptide nanotube · Self-assembly · Diffuse · H-bonds · Molecular dynamics

Introduction

Cyclic peptide nanotubes (SPNs) have attracted much attentions from the research community in recent years, for their applications in biology, chemistry and materials science [1–5].

Early in 1974, De Santis predicted the possibility of forming cylindrical structures from D, L-cyclic peptides on the basis of investigation of the structural characteristics of linear polypeptides [6]. While early experiments could not verify the existence of any such nanotube assembly, Ghadiri and his group synthesized, for the first time, the hollow tubular structures in 1993 [7–8]. A number of investigations were made on the syntheses, characterization and specific functional applications of cyclic peptide nanotubes. These work involved needle-shaped microcrystals as large as 200 μm, prepositioned dimers crystals, self-assembly embedded in lipid bilayers, antibacterial cyclic peptide, cyclic peptide with hydrophobic inner surfaces and so on [9–14]. These investigations highlight the use of cyclic peptide nanotubes as models for mimicking bioloical channels, molecular adapters for pore-forming proteins, transport vehicles in drug delivery systems and other nanostructural materials [15–20]. Some theoretical studies by ab initio, semiempirical approaches and molecular dynamics (MD) have also been performed to reveal the importance of channels in sustaining biological systems and their potential utility in nanotechnology and biomaterials [21–26]. All these work made the structure-property relationship of channels an active area of investigation [27–31].

SPNs are prone to congregate, and so it is difficult to characterize their structures and properties. Therefore, some investigators adopted *N*-alkylation substituents on alternating amino acid residues to stop the self-assembly at the dimer stage to increase their solubility [32–33]. For example, Thomas D. Clark et al. [11], synthesized and self-assembled 20 cyclic peptide dimers through backbone *N*-alkylation. Although this method can be used to quickly obtain some information, it was not confirmed through experiments whether cyclic peptides can be made nanotubes by stretching. Engels [34] and Tarek [35] investigated the behaviors of H_2O molecules in octapeptide nanotubes of cyclo[-(Gln-D-Ala-G1u-L-Ala-)$_4$] and cyclo[(L-Trp-D-Leu)$_3$-L-Gln-D-Leu] by MD and revealed some mechanics of longer nanotubes, but they did not study the behaviors of H_2O in nanotubes with different diameters. Therefore, in this study, we synthesized *cyclo*[(-D-Phe-L-Ala)$_{n\ =\ 4}$-] and self-assembled it to nanotube bundles. We verified through experiment that the cyclic peptide can stretch into long nanotubes. And then, we investigated the structures of single nanotubes of *cyclo*[(-D-Phe-L-Ala)$_{n\ =\ 3,4,5,6}$-] and the motion behaviors of H_2O molecules constrained in these nanotubes. We hope this may provide evidences for their applications as sensors or transport channels.

Materials and methods

Materials systems

The elementary components of SPNs are cyclopeptides consisting of alternating chirality linear polypeptide with head connected to tail (Fig. 1a). The rings adopt a flat-ring shape conformation and the C=O and N–H groups are roughly perpendicular to the ring plane, which facilitates the rings stacking together by means of inter-rings H-bonds and self-assembling into extended hollow tubular structures (Fig. 1b).

The diameters of nanotubes change with the numbers of amino acid residues employed [11]. Studies indicated that cyclic peptides with six, eight, ten and twelve-residues are most suitable for design and application of cyclic peptide nanotubes because cyclic D, L-peptides with less than six residues have prohibitively large ring strain, peptides with more than twelve residues are too large to sample in the flat ring-shaped conformation [9]. So, we investigated four nanotubes of *cyclo*[(-D-Phe-L-Ala)$_{n\ =\ 3,4,5,6}$-] (Fig. 1a), in which $n = 3,4,5,6$ represents hexa-, octa-, deca- and dodeca-peptide respectively, and these nanotubes have different diameters.

In addition, we synthesized and characterized the cyclic octapeptides to confirm the existence of long nanotubes, because cyclic octapeptides possess the optimum balance of a low-strain ring structure and the desired flat ring-shaped conformational stability.

Experiment

As shown in Fig. 2, the experimental process consists of the synthesis of linear multipeptides, the cyclization of linear peptides, the self-assembly of cyclic peptide nanotubes and the characterization of nanotubes.

The synthesis vessel is custom-made, which includes a glass vessel with a glass frit at the bottom and a screw cap with septum on top for addition of reagents. Solvents and

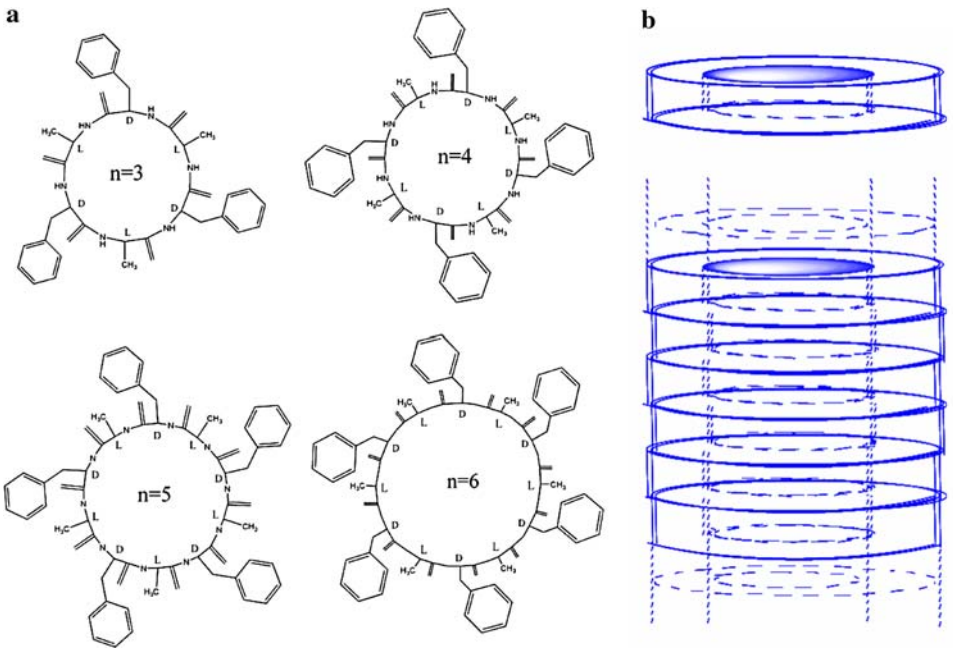

Fig. 1 Material system in investigation. (**a**) Cyclic peptide with different amino acid residues in which $n = 3,4,5,6$ represent hexa-, octa-, deca- and dode-peptide respectively. (**b**) Self-assembled nanotube from cyclic peptides

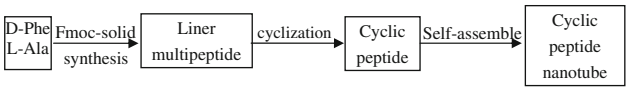

Fig. 2 Process of material synthesis: D-Phe and L-Ala was alternately connected to linear multipeptide according to Fmoc solid phase peptide synthesis methods; linear multipeptide was cyclized in dilute solution; cyclic peptide self-assembled into nanotubes

soluble reagents are removed by suction. Nitrogen gas blows from bottom to up to protect and stir the reagents.

Linear multipeptide was synthesized using Fmoc solid phase peptide synthesis methods [36], cyclization of linear multipeptides was done in a dilute solution to reduce the subsidiary [13, 14], self-assembly was done in neat TEA [9], and characterization was done by mass spectrometry (MS), fourier transform infrared spectroscopy (FT-IR) and scanning electron microscopy (SEM).

Molecular modeling

There are two stacking arrangements for the rings in the nanotubes: one is parallel and the other is antiparallel. Many investigations revealed that D, K-cyclic peptide prefers an antiparallel stacking arrangement [23, 37, 38], and so the rings in our models are put in antiparallel.

The nanotubes we built are single nanotubes consisting of ten peptide rings of *cyclo*[(-D-Phe-L-Ala)$_{n\ =\ 3,4,5,6}$-]. Firstly, the single nanotubes were optimized with molecular mechanics (MM); the rms gradient is 0.001 kcal/mol. Atomic based summation method was used to calculate the long-range van der Waals interactions and the electrostatic interactions. Spline width is 1 Å, cutoff distance is 9.5 Å and buffer width is 0.5 Å. The resulting length of the nanotube is 48 Å. Then, the nanotubes were put in three-dimensional periodical boundary boxes, with axes of nanotubes parallel to axis-*a*. The parameters of periodical boxes are a = 48 Å, b = c=30 Å, $\alpha = \beta = \gamma = 90°$ respectively. Lattice-*a* equals to the lengths of nanotubes so that the terminal rings can be hydrogen-bonded with the rings in their neighboring cells. The nanotubes will stretch to a single infinite nanochannels when they repeat along axis-*a*. Both *b* and *c* are much longer than the maximum nanotube diameter 25 Å of SPN ($n = 6$). This will ensure that the H_2O molecules are not be affected by the periodic image.

Ten H_2O molecules are constrained in the nanotube. All the H_2O molecules are arranged along the centerline of the nanotubes and each H_2O molecule locates between two neighboring rings.

1.5 ns MD was applied to these nanotubes. A NVT ensemble at 298 K, a time step of 1 fs and a nose thermostat were employed for MD. Ewald method was used to calculate the long-range van der Waals interactions and the electrostatic interactions. Ewald accuracy achieved is 0.001 kcal/mol and the update width used is 3 Å. Every 1,000 fs, one structure was stored in the trajectory for analysis.

All the modeling work was conducted with Materials Studio (Accelrys Inc.) software on sgi3800 origin sever using COMPASS force field. COMPASS is an ab initio force field used to realize accurate and simultaneous prediction of gas-phase properties and condensed-phase properties for a broad range of small molecules and polymers [39–41], which fits our system.

Results and discussion

Experimental results

As are shown in Fig. 3, a peak at 873.8 (Fig. 3a) corresponds to the mass of *cyclo*[(-D-Phe-L-Ala)$_4$-], and the β-sheet nature of hydrogen bonding is supported by FT-IR spectra recorded in nanotube (Fig. 3b), which displays amide I and amide II bands at 1,632 and 1,541 cm^{-1}, respectively. These positions are typical of β-sheets [42] and similar to those found in nanotubes and dimers composed of D, L-cyclic peptides [7–11]. The hydrogen bonding by N–H is further supported by amide A bands near 3,325 cm^{-1} [43–45], while a band appearing at 3,444 cm^{-1} may correspond to the N–H band of the monomer [46].

It can be seen from the morphology of self-assembled *cyclo*[(-D-Phe-L-Ala)$_4$-] nanotube (Fig. 3c) that the nanotubes predominantly formed bundles of 6–8 μm in length and of about 200–300 nm in diameter and the largest diameter goes up to 900 nm.

It can therefore be concluded from discussions above that *cyclo*[(-D-Phe-L-Ala)$_4$-] has been synthesized and self-assembled into nanotubes, and cyclic peptides with *N*-alkylation can also form long nanotubes when substituent groups are absent if they can form dimers.

Structure of nanotube

As the nanotubes are prone to aggregate, we can see the nanotube bundles by SEM only. As a matter of fact, it is very important for us to characterize the structures and properties of single nanotubes.

The structure of *cyclo*[(-D-Phe-L-Ala)$_{n\ =\ 3,4,5,6}$] can be characterized from analyzing the MD trajectories. It can be seen from the snapshots of trajectories (Fig. 4b–e) that all the cyclic peptides adopt flat ring conformation and are hydrogen-bonded by six, eight, ten or twelve H-bonds in each neighboring rings. These H-bonds stacking makes the nanotubes very stable. The hydrogen-bonding distance (N···O) between neighboring peptide rings of Phe is 2.9–3.1 Å and the distance between neighboring rings of

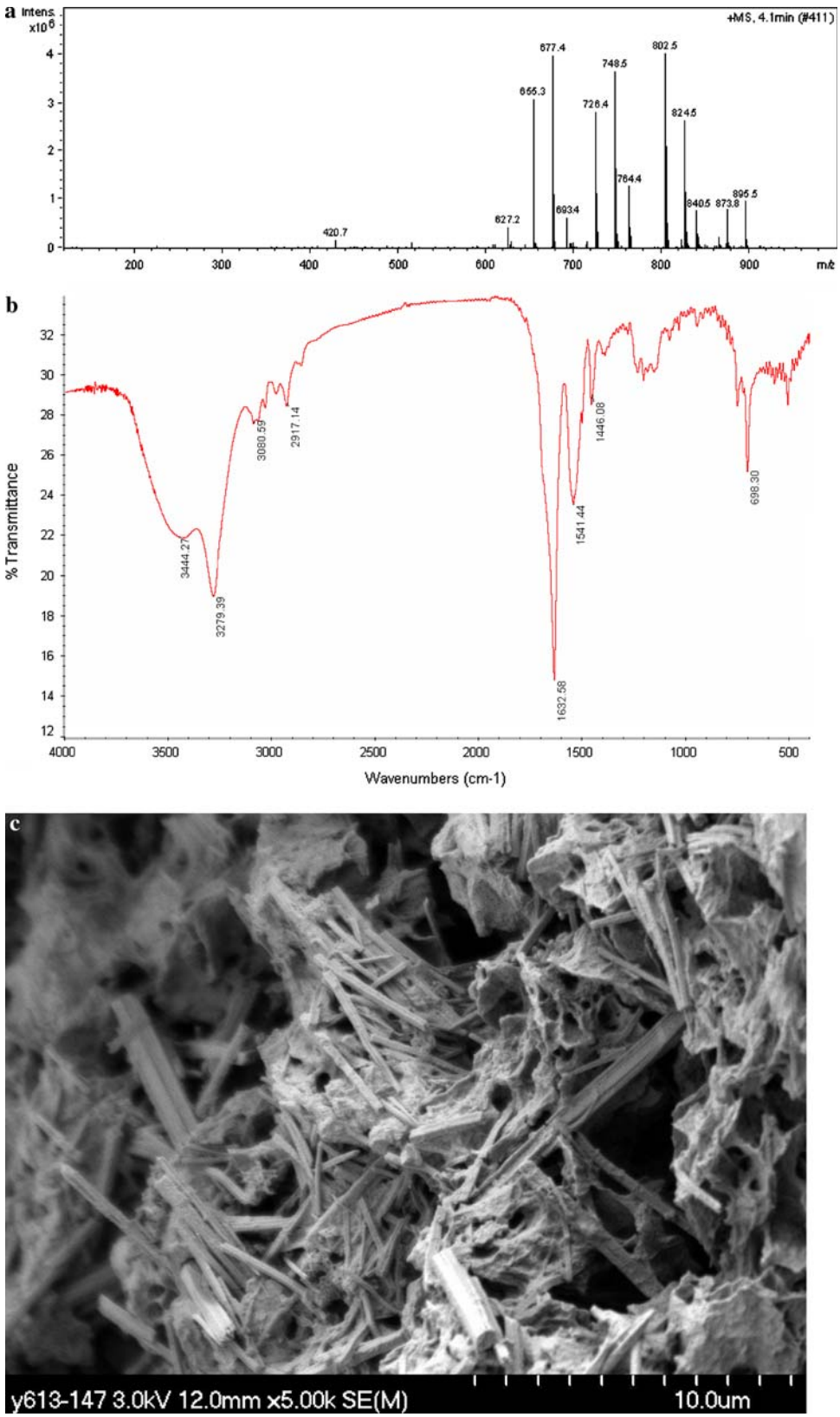

Fig. 3 MS, FT-IR and SEM results. (**a**) MS spectrum of *cyclo*[(-D-Phe-L-Ala)$_4$-]. (**b**) FT-IR spectrum of self-assembled nanotubes of *cyclo*[(-D-Phe-L-Ala)$_4$-]. (**c**) SEM of self-assembled nanotubes of *cyclo*[(-D-Phe-L-Ala)$_4$-]

Ala is 2.8–3.2 Å for all the nanotubes with different n, which is consistent with the experimental results presented in [7]. The average distance between the centroids of neighboring rings in the four models are within the range of 4.5–5.2 Å, which is also in agreement with experimental results presented in [9].

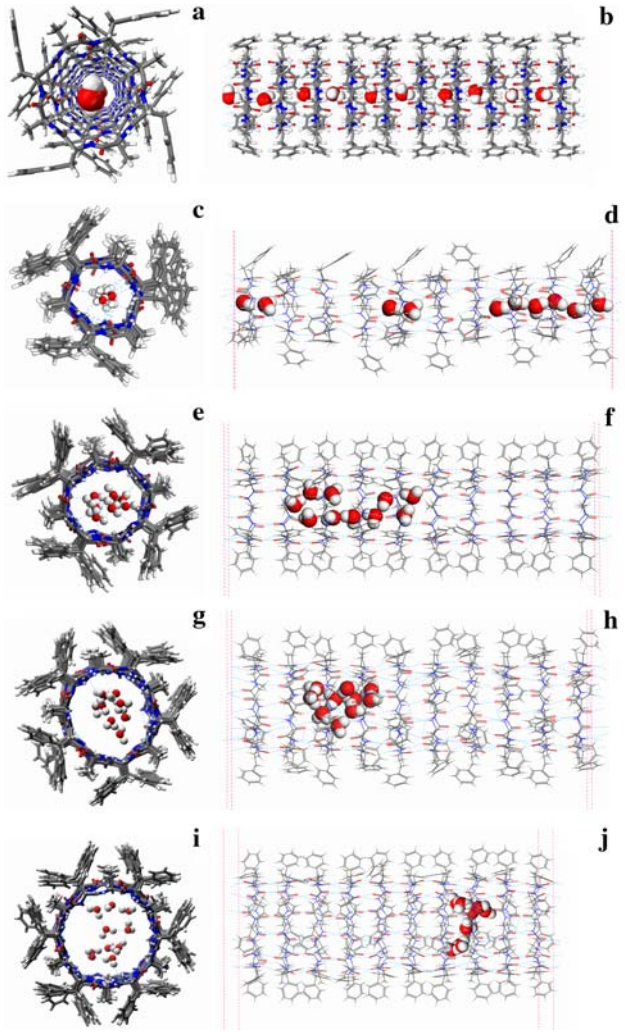

Fig. 4 Single nanotube models. (**a**, **b**) Initial model of single nanotube (cyclic octapeptide), in which each H_2O locates between two neighboring rings. (c–j) Snapshots of single hexa-(**c**, **d**), octa-(**e**, **f**), deca-(**g**, **h**) and dode-(**i**, **j**) cyclopeptide nanotubes after 1.5 ns MD simulation, in which H_2O molecules congregate. (**a**, **c**, **e**, **g** and **i**) top view and (**b**, **d**, **f**, **h** and **j**) side view

The diameters of nanotubes can be measured from the profiles of concentration distribution of lateral nanotube (Fig. 5). The internal diameter is the distance between two main peaks and the outer diameter is the width of the profile.

It can be seen from Table 1 that the calculated inner diameters are 5.9 Å, 8.1 Å, 10.8 Å and 13.1 Å and the outer diameters are 18.2 Å, 21.7 Å, 23.4 Å and 25.9 Å for $n = 3, 4, 5$ and 6 respectively, of which the inner diameters of nanotubes with $n = 4$, 5 and 6 are consist with the experimental values presented in [47, 48, 8]. This means that our optimum structures are reasonable.

Distribution of H_2O in nanotubes

The distribution of H_2O molecules in the channels is directly related to the diameters of nanotubes. In general,

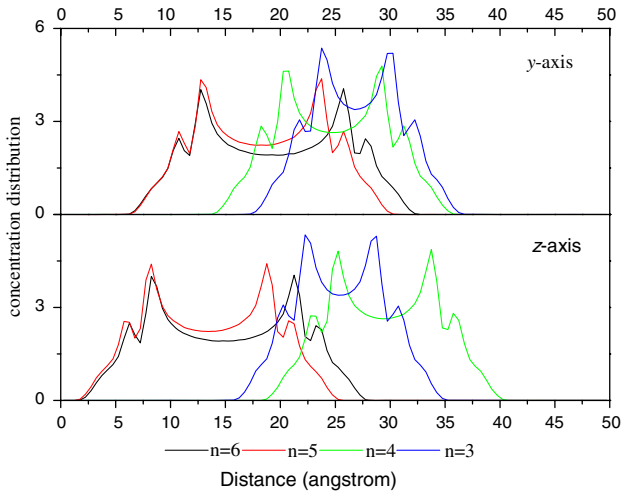

Fig. 5 Concentration distribution of each nanotube along *y*- and *z*-axis. In each profile, the distance between two main peaks represents the internal diameter and the width of the profile is the outer diameter. The internal diameter are about 5.9 Å, 8.1 Å, 10.8 Å and 13.1 Å, and the outer diameters are about 18.2 Å, 21.7 Å, 23.4 Å and 25.9 Å for $n = 3$, 4, 5 and 6 respectively

H_2O molecules incline to form H-bonds and aggregate in lateral direction priority; only if there is no space, they aggregate along axial nanotubes.

The distribution of atomic concentration can demonstrate the spatial distribution of molecules. We compared the initial, final and average concentrations of H_2O molecules and nanotubes by analyzing the MD trajectories. It can be seen from the profiles of decapeptide shown in Fig. 6 that the nanotubes distribute evenly along *x*-axis and concentrate in a range of lengths along *y*-axis and *z*-axis. These nanotubes remain very stable all the time, while the atomic concentrations of H_2O molecules changes largely. In the initial models, H_2O molecules distribute evenly along *x*-axis and position at the center of nanotube along *y*-axis and *z*-axis. In the final models, H_2O molecules concentrate in a certain range of lengths along *x*-axis and distribute evenly within a range of nanotubes along *y*-axis and *z*-axis, which indicates that H_2O molecules rearranged and aggregated along *x*-axis. It can be seen from the average distribution of H_2O molecules and nanotubes in the whole MD process that H_2O molecules distribute evenly

Table 1 Calculated and experimental diameters of inner and outer nanotubes

n		3	4	5	**6**
Diameters (Å)	Inner	5.9	8.1	10.8	13.1
		–	7[a]	10[b]	13[c]
	Outer	18.2	21.7	23.4	25.9

Experimental values a from Ref. [47], b from Ref. [48], c from Ref. [8]

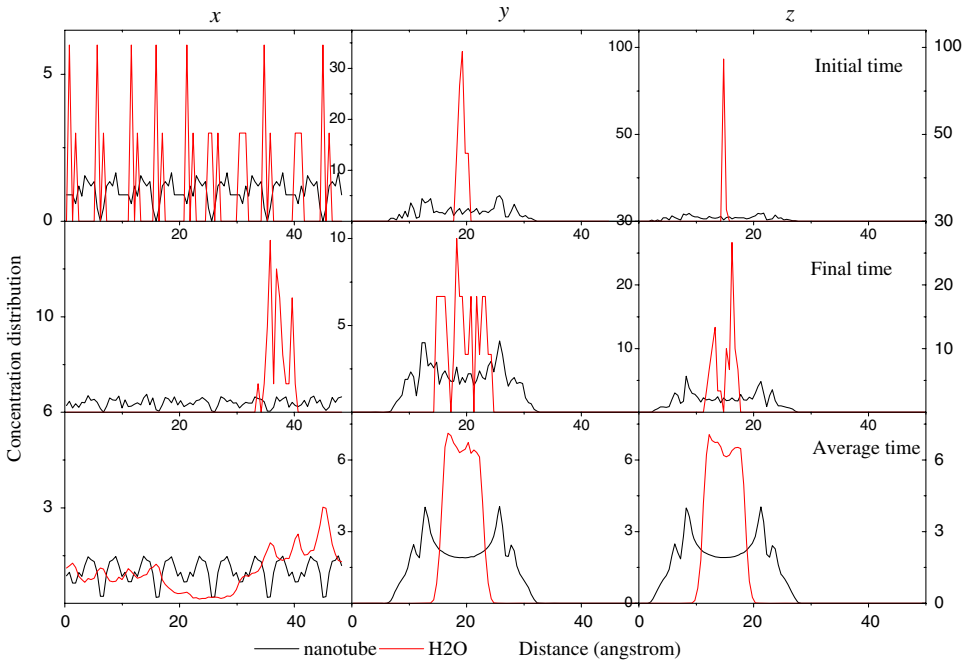

Fig. 6 Concentration distribution profiles of H_2O molecules and nanotube in initial, final and average models. H_2O molecules aggregate along *x*-axis and distribute evenly within the ranges of nanotube along *y*-axis and *z*-axis at the final, but they distribute evenly within the ranges of nanotube on average

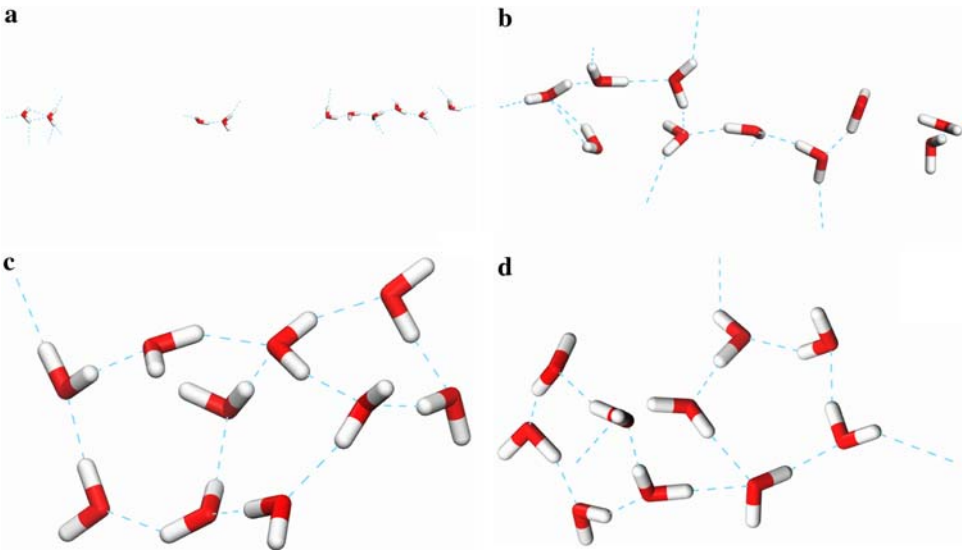

Fig. 7 The arrangement of H_2O molecules confined in the nanotube. (**a**) $n = 3$. (**b**) $n = 4$. (**c**) $n = 5$. (d) $n = 6$. The dash lines represent H-bonds

within a range of nanotubes along *y*-axis, *z*-axis and *x*-axis, which indicate that H_2O molecules diffuse in the whole nanotube.

The diffusion of H_2O molecules in cyclic peptide nanotubes is different from that of H_2 molecules and alkyl lines in carbon nanotubes. In carbon nanotubes, H_2 molecules and alkyl lines are adsorbed to the walls of nanotubes [49, 50]. While H_2O molecules in cyclic peptide nanotubes tend to aggregate with each other by H-bonds, because the H-bonding interaction between H_2O molecules is stronger than van der Waals energy between H_2O molecules and the nanotubes.

As shown in Fig. 7, most H_2O molecules in the hexapeptide ($n = 3$) nanotube arrange in line with H-bonds linked, and there is a single water molecule located on the tube axis. The H_2O molecules in octapeptide ($n = 4$) stack in layers of one and two water molecules, which is similar to Engels' and Tarek' results [35, 36]. From the arrangement of $n = 4$ we can see that the H_2O molecules inside the cyclic peptide nanotubes have similar arrangements no matter the single nanotubes are in solvent, lipid or vacuum, which indicate that the environment outside the nanotubes molecules has little effect on the cyclic peptide nanotubes. We can thus also deduce the arrangements of H_2O

molecules in the decapeptide and dodecapeptide nanotubes ($n = 5, 6$). We found through simulation that the H_2O molecules in both decapeptide and dodecapeptide nanotubes tend to form circularities with H-bonding, and their stability improves as they diffuse along the channels.

Movement of H_2O molecules in nanotube

It is well-known that the ion transport rate of cyclic peptide nanotube is three times faster than that of gramicidin A (GA) with the similar structure [8], so it is very important to investigate the movement of H_2O molecules in nanotube.

One dimensional diffusion of H_2O

The translational mobility of H_2O can be given by calculating the mean square displacement (MSD) of the mass centre of particles, which can be expressed as follows:

$$G(r) = \left\langle \left| \vec{r}(t + t_0) - \vec{r}(t_0) \right|^2 \right\rangle$$

where $G(r)$ denotes MSD, t denotes the correlation time, and $\vec{r}$ stands for the coordinate vector of the mass of molecules.

The mean square displacements of H_2O was calculated in the longitudinal (x-axis) direction and the lateral (y- and z-axis) directions, respectively. As shown in Fig. 8, that total MSD is nearly in superposition with MSD_x, while MSD_y and MSD_z are approximatively zero. The MSD of H_2O in a cyclic peptide nanotube demonstrate the movement of H_2O molecules along x-axis, is an one dimensional diffusion in the nanotube.

In our models, the periodic boundary causes the H_2O molecules to enter to the neighboring cell after they move from 0 Å to 50 Å and their coordinate vector restarts from 0 Å. So the curves of MSD decline if the molecules go into the neighboring cell. There is no decline in models with $n = 3$ and $n = 4$ because it takes fairly long for the molecules to move out completely from one cell and enter another. It can be seen from the model with $n = 5$ that the curves decline after 600 ps because the nanotube has a larger diameter so that the molecules can be arranged in a shorter length, which enables the H_2O molecules to move out from the initial cell in a shorter period of time. Especially in model with $n = 6$, the curves exhibit fluctuation, indicate the molecules move between the cells again and again.

However, the H_2O molecules only diffuse along x-axis in the nanotube (one-dimension movement) although the diameters of nanotube are large enough to accommodate several molecules in lateral.

Coordinated motion of H_2O molecules

The even distribution of H_2O molecules in the whole MD process, and their aggregation at the end of MD process, cause the molecules to diffuse along the whole nanotube. In order to further investigate the motion of H_2O molecules in the cyclic peptide nanotube, we analyzed the instantaneous concentrations of H_2O molecules at various time (Fig. 9).

Since the H_2O molecules in the nanotube exhibit an unidimensional diffusion as discussed in section above, we only analyzed the distributions of concentrations along

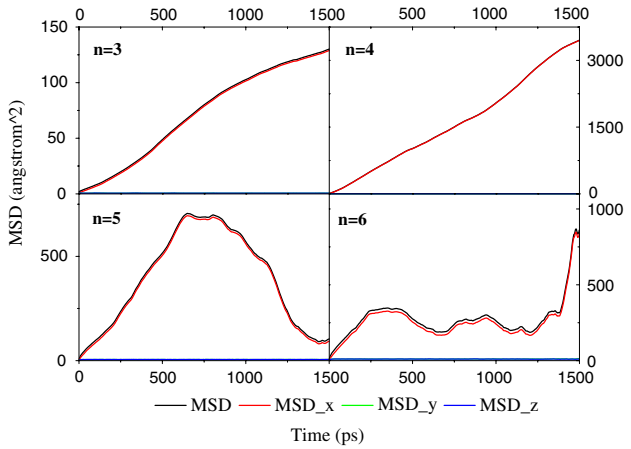

Fig. 8 MSD of H_2O molecules constrained in the peptide nanotubes of *cyclo*[(-D-Phe-L-Ala)$_{n\ =\ 3,4,5,6}$-]. The curves decline in models with $n = 5$ and $n = 6$ due to the coordinate vector of H_2O molecules restarts from 0 Å after H_2O molecules move from 0 Å to 50 Å. Total MSD is in superposition with MSD_x nearly, while MSD_y and MSD_z are approximatively zero

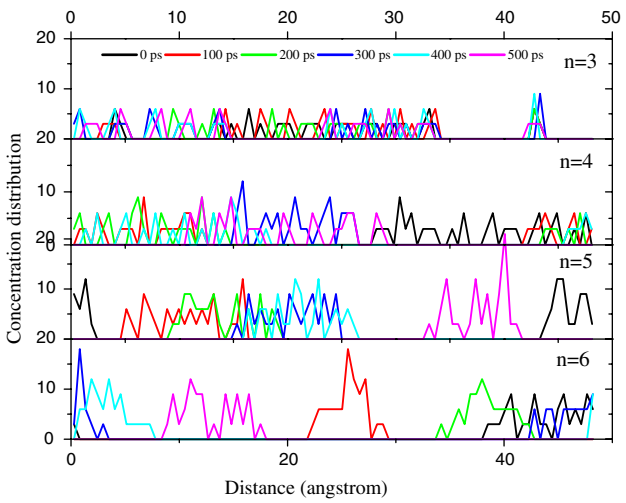

Fig. 9 Instantaneous concentration distribution of H_2O molecules in different nanotubes. In each nanotube, the curves have the same profile at different time. The curves can shift to the right or the left liberally at the next time

x-axis in this paper. In addition, considering the constraint of periodic boundary, we selected a period of time only, during which the H_2O molecules diffused across the whole length of lattice-*a* from the four trajectories.

As shown in Fig. 9, the H_2O molecules in each nanotube, have similar profiles at different time, which indicates the H_2O molecules move in cooperation. In addition, we can also see that the profiles can shift to the right or the left at the next time, which indicates H_2O molecules did not diffuse in orientation. The antiparallel ring stacking arrangement makes the whole nanotube have no polar, and the H_2O molecules can diffuse freely along the nanotube. An external forces must be exerted for H_2O molecules to move unilaterally.

Conclusion

Peptide nanotube of *cyclo*[(-D-Phe-L-Ala)$_{n\,=\,4}$-] was synthesized and self-assembled to nanotubes in experiment. The structures of nanotubes of *cyclo*[(-D-Phe-L-Ala)$_{n\,=\,3,4,5,6}$-] and the motion behaviors of H_2O molecules in these nanotubes were investigated by molecular dynamics. Experimental results show that *cyclo*[(-D-Phe-L-Ala)$_{n\,=\,4}$-] peptides self-assemble into nanotube bundles of 6–8 μm in length and of about 200–300 nm in diameter. Molecular modeling results show that single nanotubes of *cyclo*[(-D-Phe-L-Ala)$_{n\,=\,3,4,5,6}$-] are very stable, in which hydrogen-bonding distances (N···O) between neighboring peptide rings of Phe is 2.9–3.1 Å and the distance of Ala is 2.8–3.2 Å. The average distance between centrio of neighboring rings is within range of 4.5–5.2 Å. The internal diameters of these nanotubes are 5.9 Å, 8.1 Å, 10.8 Å and 13.1 Å and the outer diameters are 18.2 Å, 21.7 Å, 23.4 Å and 25.9 Å for $n = 3$, 4, 5 and 6 respectively. Molecular modeling results indicate that H_2O molecules move in cooperation in single nanotube and they diffuse in one dimension, but they did not diffuse unilaterally due to the antiparallel ring stacking arrangement. It needs driving force for H_2O molecules to transport through the nanotube unilaterally.

References

1. Hartgerink JD, Clark TD, Ghadiri MR (1998) Peptide nanotubes and beyond. Chem Eur J 4:1367–1372
2. Brea RJ, Vazquez ME, Mosquera M, Castedo L, Granja JR (2007) Controlling multiple fluorescent signal output in cyclic peptide-based supramolecular systems. J Am Chem Soc 129:1653–1657
3. Janshoff A, Dancil KPS, Steinem C, Greiner DP, Lin VSY, Gurtner C, Motesharei K, Sailor MJ, Ghadiri MR (1998) Macroporous p-type silicon Fabry-Perot layers. Fabrication, characterization, and applications in biosensing. J Am Chem Soc 120:12108–12116
4. David G, Pierre BM (2001) Self-assembly of cyclic peptides into nanotubes and then into highly anisotropic crystalline materials. J Angew Chem Int Ed 40:4635–4638
5. Ghadiri MR (1995) Self-assembled nanoscale tubular ensembles. Adv Mater 7:675–677
6. De Santis P, Morosetti S, Rizzo R (1974) Conformational analysis of regular enantiomeric sequences. Macromolecules 7:52–58
7. Ghadiri MR, Granja JR, Milligan RA, McRee DE, Khazanovich N (1993) Self-assembling organic nanotubes based on a cyclic peptide architecture. Nature 366:324–327
8. Ghadiri MR, Granja JR, Buehler LK (1994) Artificial transmembrane ion channels from self-assembling peptide nanotubes. Nature 369:301–304
9. Hartgerink JD, Granja JR, Milligan RA, Ghadiri MR (1996) Self-assembling peptide nanotubes. J Am Chem Soc 118:43–50
10. Kim HS, Hartgerink JD, Ghadiri MR (1998) Oriented self-assembly of cyclic peptide nanotubes in lipid membranes. J Am Chem Soc 120:4417–4424
11. Clark TD, Buriak JM, Kobayashi K, Isler MP, McRee DE, Ghadiri MR (1998) Cylindrical beta-sheet peptide assemblies. J Am Chem Soc 120:8949–8962
12. Fernandez-Lopez S, Kim HS, Choi EC, Delgado M, Granja JR, Khasanov A, Kraehenbuehl K, Long G, Weinberger DA, Wilcoxen KM, Ghadiri MR (2001) Antibacterial agents based on the cyclic D, L-alpha-peptide architecture. Nature 412:452–455
13. Amorin M, Castedo L, Granja JR (2003) New cyclic peptide assemblies with hydrophobic cavities, The structural and thermodynamic basis of a new class of peptide nanotubes. J Am Chem Soc 125:2844–2845
14. Brea RJ, Lopez-Deber MP, Castedo L, Granja JR (2006) Synthesis of omega-(hetero)arylalkynylated alpha-amino acid by sonogashira-type reactions in aqueous media. J Org Chem 71:7870–7873
15. Sanchez-Quesada J, Ghadiri MR, Bayley H, Braha O (2000) Cyclic peptides as molecular adapters for a pore-forming protein. J Am Chem Soc 122:11757–11766
16. Clark TD, Buehler LK, Ghadiri MR (1998) Self-assembling cyclic beta(3)-peptide nanotubes as artificial transmembrane ion channels. J Am Chem Soc 120:651–656
17. Horne WS, Ashkenasy N, Ghadiri MR (2005) Modulating charge transfer through cyclic D,L-alpha-peptide self-assembly. Chem Eur J 11:1137–1144
18. Ortiz-Acevedo A, Xie H, Zorbas V, Sampson WM, Dalton AB, Baughman RH, Draper RK, Musselman IH, Dieckmann GR (2005) Diameter-selective solubilization of single-walled carbon nanotubes by reversible cyclic peptides. J Am Chem Soc 127:9512–9517
19. Christoph AS (2004) Elements for the construction of molecular devices: template effects and self-assembly. J Phys Org Chem 17:967–972
20. Ashkenasy G, Ghadiri MR (2004) Boolean logic functions of a synthetic peptide network. J Am Chem Soc 126:11140–11141
21. Lewis JP, Pawley NH, Sankey OF (1997) Theoretical investigation of the cyclic peptide system cyclo[(D-Ala-Glu-D-Ala-Gln)$_{(m=1-4)}$]. J Phys Chem B 101:10576–10583
22. Jishi RA, Flores RM, Valderrama M, Lou L, Bragin J (1998) Equilibrium geometry and properties of cyclo[(Gly-D-Ala)$_4$] and {cyclo[(Gly-D-Ala)$_4$]}$_2$ from density functional theory. J Phys Chem A 102:9858–9862
23. Chen G, Su S, Liu R (2002) Theoretical studies of monomer and dimer of cyclo [(L-Phe^1-D-Ala^2)$_n$] and cyclo[(-L-Phe^1-D-^{Me}N-Ala^2)$_n$](n=3-6). J Phys Chem B 106:1570–1575

24. Khurana E, Nielsen SO, Ensing B, Klein ML (2006) Self-assembling cyclic peptides, molecular dynamics studies of dimers in polar and nonpolar solvents. J Phys Chem B 110:18965–18972
25. Hwang H, Schatz GC, Ratner MA (2006) Steered molecular dynamics studies of the potential of mean force of a Na^+ or K^+ ion in a cyclic peptide nanotube. J Phys Chem B 110:26448–26460
26. Hwang H, Schatz GC, Ratner MA (2006) Ion current calculations based on three dimensional Poisson-Nernst-Planck theory for a cyclic peptide nanotube. J Phys Chem B 110:6999–7008
27. Clark TD, Ghadiri MR (1995) Supramolecular design by covalent capture. design of a peptide cylinder via hydrogen-bond-promoted intermolecular olefin metathesis. J Am Chem Soc 117:12364–12365
28. Rosenthal-Aizman K, Svensson G, Unden A (2004) Self-assembling peptide nanotubes from enantiomeric pairs of cyclic peptides with alternating D and L amino acid residues. J Am Chem Soc 126:3372–3373
29. Dawson PE, Churchill MJ, Ghadiri MR, Kent SBH (1997) Modulation of reactivity in native chemical ligation through the use of thiol additives. J Am Chem Soc 119:4325–4329
30. Ranganathan D (2001) Designer hybrid cyclopeptides for membrane ion transport and tubular structures. Acc Chem Res 34:919–930
31. Bong DT, Ghadiri MR (2001) Self-assembling cyclic peptide cylinders as nuclei for crystal engineering. Angew Chem Int Edit 40:2163–2166
32. Horne WS, Stout CD, Ghadiri MR (2003) A heterocyclic peptide nanotube. J Am Chem Soc 125:9372–9376
33. Horne WS, Yadav MK, Stout CD, Ghadiri MR (2004) Heterocyclic peptide backbone modifications in an α-helical coiled coil. J Am Chem Soc 126:15366–15367
34. Engels M, Bashford D, Ghadiri MR (1995) Structure and dynamics of self-assembling peptide nanotubes and the channel-mediated water organization and self-diffusion. a molecular dynamics study. J Am Chem Soc 117:9151–9158
35. Tarek M, Maigret B, Chipot C (2003) Molecular dynamics investigation of an oriented cyclic peptide nanotube in DMPC bilayers. Biophys J 85:2287–2298
36. Wang SS, Makofske R, Bach A (1980) Automated solid phase synthesis of thymosinal. Int J Pept Protein Res 15:1–4
37. Kobayashi K, Granja JR, Ghadiri MR (1995) Beta-sheet peptide architecture: measuring the relative stability of parallel vs. antiparallel beta-Sheets. Angew Chem Int Ed 34:95–98
38. Ghadiri MR, Kobayashi K, Granja JR, Chadha RK, McRee DE (1995) The structural and thermodynamic basis for the formation of self-assembled peptide nanotubes. Angew Chem Int Ed 34: 93–95
39. Sun H (1995) Ab initio calculations and force field development for computer simulation of polysilanes. Macromolecules 28: 701–712
40. Sun H (1998) COMPASS: an ab initio force-field optimized for condensed-phase applications – overview with details on alkane and benzene compounds. J Phys Chem B 102:7338–7364
41. Sun H, Ren P, Fried JR (1998) The COMPASS force field: parameterization and validation for polyphosphazenes. Comput Theor Polym Sci 8:229–246
42. Krimm S, Bandekar J (1986) Vibrational spectroscopy and conformation of peptides, polypeptides, and proteins. Adv Protein Chem 38:181–364
43. Pavone V, Benedetti E, Blasio BD, Lombardi A, Pedone C, Tomasich L, Lorenzi GP (1989) Regularly alternating L, D-peptides. III. Hexacyclic peptides from valine or phenylalanine. Biopolymers 28:215–223
44. Sun X, Lorenzi GP (1994) On the stacking of β-rings: the solution self-association behavior of two partially *N*-methylated cyclo(hexaleucines). Helv Chim Acta 77:1520–1526
45. Bandekar J (1992) Amide modes and protein conformation. Biochim Biophys Acta 1120:123–143
46. Saviano M, Lombardi A, Pedone C, Blasio BD, Sun XC, Lorenzi GP (1994) A structural two-ring version of a tubular stack of β-rings in crystals of a cyclic D,L-hexapeptide. J Incl Phenom 18:27–36
47. Granja JR, Ghadiri MR (1994) Channel-mediated transport of glucose across lipid bilayers. J Am Chem Soc 116:10785–10786
48. Khazanovich N, Granja JR, McRee DE, Milligan RA, Ghadiri MR (1994) Nanoscale tubular ensembles with specified internal diameters. Design of a self-assembled nanotube with a 13 angstrom. pore. J Am Chem Soc 116:6011–6012
49. Cheng HS, Cooper AC, Pez GP, Kostov MK, Piotrowski P, Stuart SJA (2005) Molecular dynamics simulations on the effects of diameter and chirality on hydrogen adsorption in single walled carbon nanotubes. J Phys Chem B 109:3780–3786
50. Yang H, Liu Y, Zhang H, Li ZS (2006) Diffusion of single alkane molecule in carbon nanotube studied by molecular dynamics simulation. Polymer 47:7607–7610